Chapter 15
Hume–Rothery Stabilization Mechanism in Low-Temperature Phase Zn_6Sc Approximant and e/a Determination of Sc and Y in M–Sc and M–Y (M = Zn, Cd and Al) Alloy Systems

U. Mizutani, M. Inukai, H. Sato, and E.S. Zijlstra

Abstract We have performed FLAPW electronic structure calculations with subsequent FLAPW-Fourier analysis for the low temperature phase Zn_6Sc containing 336 atoms per unit cell with space group B2/b. The square of the Fermi diameter $(2k_F)^2$, electrons per atom ratio **e**/**a** and *critical* reciprocal lattice vector $|\mathbf{G}|^2$s were determined. The origin of its pseudogap at the Fermi level was interpreted as arising from interference of electrons with $(2k_F)^2 = 79.0 \pm 0.2$ with sets of lattice planes with $|\mathbf{G}|^2$ ranging over 72 to 96. The work was extended to intermetallic compounds existing in M–Sc and M–Y (M = Zn, Cd and Al) binary alloy systems. The effective **e**/**a** values for Sc and Y were deduced to be 3.0 and 3.1, respectively.

15.1 Introduction

Guided by the empirical Hume–Rothery electron concentration rule, Tsai and his coworkers discovered a series of thermally stable Al–Cu–TM (TM = Fe, Ru and Os) and Al–Pd–TM (TM = Mn, Re) icosahedral quasicrystals in the early 1990s [1, 2]. Here negative valences proposed by Raynor [3] for transition metal (TM) elements were used. Tsai et al. [4] reported in 2000 that a stable binary icosahedral quasicrystal can be formed at the composition $Cd_{5.7}Yb$ and belongs to a new class of packing 66-atom icosahedral clusters. They also revealed that the compound Cd_6Yb lying next to the quasicrystal above in the phase diagram corresponds to its

U. Mizutani (✉)
Nagoya Industrial Science Research Institute, 1-13 Yotsuya-dori, Chikusa-ku, Nagoya 464-0819, Japan
e-mail: uichiro@sky.sannet.ne.jp

M. Inukai
Toyota Technological Institute, Hisakata, Tempaku-ku, Nagoya 468-8511, Japan

H. Sato
Aichi University of Education, Kariya-shi, Aichi 448-8542, Japan

E.S. Zijlstra
Theoretical Physics, University of Kassel, 34132 Kassel, Germany

1/1–1/1–1/1 approximant with space group $Im\bar{3}$. More recently, Ishimasa and his associates [5] have succeeded in synthesizing the Zn–Mg–Sc quasicrystal guided by the work of Andrusyak et al. [6]. Later, Ishimasa et al. [7] studied the structures in more details in both quasicrystals and their 1/1–1/1–1/1 approximants in Zn–Mg–Sc, Cu–Ga–Mg–Sc and Zn–Mg–Ti alloys and revealed the presence of a few Zn atoms in the first shell in the 1/1–1/1–1/1 approximants and claimed them to be isostructural to the family of Cd_6M (M = Yb and Ca) 1/1–1/1–1/1 approximants. They also discussed the formation range for the Tsai-type icosahedral quasicrystals in terms of electrons per atom ratio $\mathbf{e/a}$ by taking a composition average of $(\mathbf{e/a})$ values of constituent elements: $(\mathbf{e/a})_{Cu} = (\mathbf{e/a})_{Ag} = 1.0$, $(\mathbf{e/a})_{Mg} = (\mathbf{e/a})_{Ca} = (\mathbf{e/a})_{Zn} = (\mathbf{e/a})_{Cd} = (\mathbf{e/a})_{Yb} = 2.0$, $(\mathbf{e/a})_{Sc} = (\mathbf{e/a})_Y = 3.0$ and $(\mathbf{e/a})_{Ti} = 4.0$. As a result, they are commonly stabilized at $\mathbf{e/a}$ ranging over 2.00 to 2.15. It is worthwhile noting, at this stage, that tri-valence for Sc and Y in Group 3 and quadri-valence for Ti and Zr in Group 4 in the periodic table were originally proposed by Pauling [8].

There is a clear difference in the approach between Pauling and Raynor: Pauling treated the valence band of the TM element itself to define its metallic valence, while Raynor considered the effective $\mathbf{e/a}$ of the TM element embedded in the host metal Al. Obviously, a substantial difference in the electron concentration parameter emerged between them. In the past, experimentalists have employed either of these two models upon discussing the $\mathbf{e/a}$-dependent alloy phase stability or the Hume–Rothery electron concentration rule, though both models were constructed without any rigorous justification based on first-principles electronic structure calculations. To overcome this difficulty, Mizutani and coworkers [9–11] employed first-principles FLAPW (Full potential Linearized Augmented Plane Wave) electronic structure calculations and established a powerful technique to extract Fs–Bz (Fermi surface–Brillouin zone) interactions involved and to determine the $\mathbf{e/a}$ value for elements and intermetallic compounds, regardless of whether or not the TM element is involved. They have made full use of its formalism, in which the wave functions outside the muffin-tin (MT) spheres are expanded into plane waves over allowed reciprocal lattice vectors $\mathbf{G}$.

The Zn_6Sc compound is known to be the 1/1–1/1–1/1 approximant to its quasicrystal and the structure of its low temperature phase has been recently determined by Ishimasa et al. [12]. The geometrically disordered atom cluster in the first shell undergoes an orientational ordering and the structure was described as a perfectly ordered phase containing a total of 336 atoms per a monoclinic unit cell with space group $C2/c$. In the present work, we have performed the WIEN2k-FLAPW band calculations with subsequent FLAPW-Fourier analysis for Zn_6Sc with equivalent space group $B2/b$. The calculations above were extended to existing intermetallic compounds in M–Sc and M–Y (M = Al, Zn and Cd) alloy systems to determine theoretically the $\mathbf{e/a}$ values of the TM elements Sc and Y.

15.2 Electronic Structure Calculations

FLAPW band calculations have been performed by employing the commercially available WIEN2k-FLAPW program package [13] with INTEL version Linux personal computers. Our in-house Fortran90 Program has been devised to carry out the FLAPW-Fourier analysis by using "case.output1" file generated by running WIEN2k [9–11].

The FLAPW-Fourier spectrum was first constructed to plot the energy dependence of plane wave components specified by the square of reciprocal lattice vector $|\mathbf{G}|^2$ in units of $(2\pi/a)^2$ at selected symmetry points of the Brillouin zone. This allows us to extract electronic states dominating at the Fermi level. The reciprocal lattice vectors thus extracted are called *critical*. As a next step, we construct the energy dispersion relation for the LAPW state $\{2|\mathbf{k}_i + \mathbf{G}|\}^2_{E_j}$ having the largest Fourier coefficient for a given energy E_j and wave vector $\mathbf{k}_i$ produced by partitioning the Brillouin zone into $N_\mathbf{k}$ meshes. This is done in an energy interval $E_j < E < E_j + \square E$ for all $\mathbf{k}_i$ values in the Brillouin zone with subsequent averaging of $\{2|\mathbf{k}_i + \mathbf{G}|\}^2_E$ over the Brillouin zone. It provides the energy dispersion relation reflecting the LAPW states having the largest Fourier coefficient. We specifically call this the Hume–Rothery plot since it allows us to determine the square of the effective Fermi diameter $(2k_F)^2$ and the $\mathbf{e}/\mathbf{a}$ values for each intermetallic compound studied [9–11].

The WIEN2k was run by using the cut-off parameter $R_{MT}K_{max} = 6.0$, which determines the number of basis functions or size of the matrices, and $N_\mathbf{k} = 400$ for Zn_6Sc.

15.3 Results and Discussions

The energy dispersion relations and the total DOS for Zn_6Sc are shown in Fig. 15.1. A deep DOS pseudogap is formed at the Fermi level. The Zn- and Sc-partial DOSs in Zn_6Sc are shown in Figs. 15.2(a) and (b), respectively. Orbital hybridization effects mainly due to Zn-sp and Sc-d states are apparently responsible for opening a pseudogap across the Fermi level. We can alternatively discuss the origin of a pseudogap at the Fermi level in terms of Fs–Bz interactions by analyzing both FLAPW-Fourier and the Hume–Rothery plot.

Figure 15.3 shows the FLAPW-Fourier spectrum at symmetry point Γ for selected $|\mathbf{G}|^2$s for Zn_6Sc. One can immediately find that LAPW waves of $|\mathbf{G}|^2 = 76$ and 80 are most densely distributed across the Fermi level. The electronic states thus extracted are called *critical*. By studying the FLAPW-Fourier spectra at symmetry points M and X as well, we conclude that electronic states at the Fermi level are dominated over $|\mathbf{G}|^2$s from 72 to 96 and that $|\mathbf{G}|^2 = 76$ and 80 are the most *critical*. Figure 15.4(a) shows the energy dependence of $\langle \sum_{\mathbf{k}+\mathbf{G}} |C_{\mathbf{k}+\mathbf{G}}|^2_{max} \rangle_E$, or briefly $\langle |C|^2_{max} \rangle_E$, which represents the square of the maximum Fourier coefficient extracted from wave function outside the MT spheres on a given energy surface $E(\mathbf{k}) = E$. The summation is carried out over equivalent zone planes. Its value at
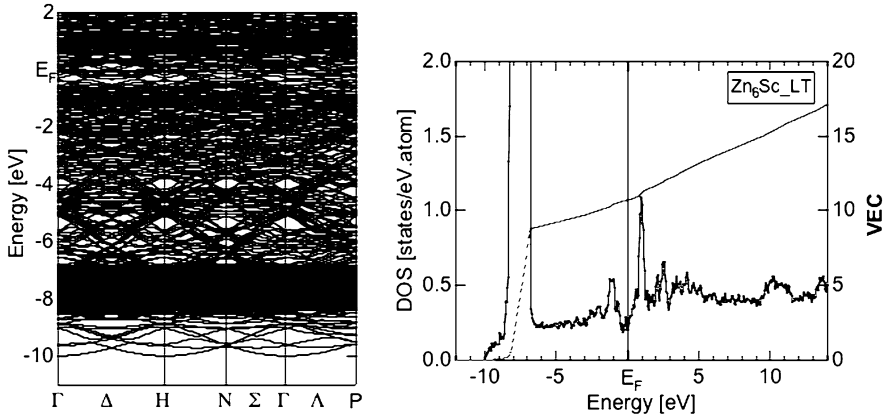
Fig. 15.1 (**a**) Dispersion relations and (**b**) total density of states (DOS) for low temperature phase Zn_6Sc. **VEC** indicates the integrated DOS or the number of electrons accommodated in the valence band
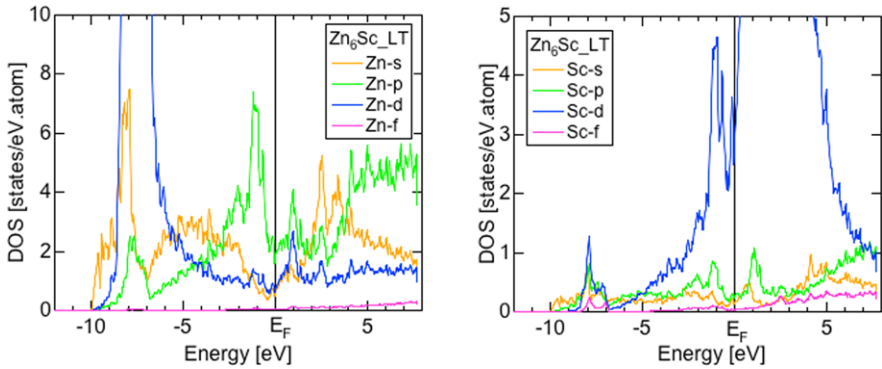

Fig. 15.2 (**a**) Zn-s, Zn-p, Zn-d and Zn-f and (**b**) Sc-s, Sc-p, Sc-d and Sc-f partial DOS of Zn_6Sc

the Fermi level, $\langle|C|^2_{max}\rangle_{E_F}$, may be used as a measure to judge the itinerancy of electrons at the Fermi level. An electron at the Fermi level is regarded as being itinerant if $\langle|C|^2_{max}\rangle_{E_F} > 0.1$ [14]. The value for Zn_6Sc turns out to be 0.067, indicating that electrons at the Fermi level are localized.

The Hume–Rothery plot and its non-dimensional standard deviation $F(E)$ [14] for Zn_6Sc are shown in Fig. 15.4(b). The data points fall on a straight line, provided that the free electron model holds well. A triangle shaped anomaly at about -8 eV reflects the highly localized Zn-3d band. One can also see that anomalies due to Sc-d states occur across the Fermi level but are well suppressed. A straight line can be drawn through the Fermi level, as indicated in Fig. 15.4(b). The square of the Fermi diameter, $(2k_F)^2$ in units of $\{2\pi/(abc)^{1/3}\}^2$, is deduced to be 79.0 ± 0.2. It is clear that the matching condition $(2k_F)^2 = |\mathbf{G}|^2$, which plays a key role in the formation of a pseudogap at the Fermi level, is well satisfied, since $(2k_F)^2$ thus obtained agrees

Fig. 15.3 FLAPW-Fourier spectrum at symmetry point G with $|\mathbf{G}|^2$s ranging over 68 to 96 for Zn_6Sc. The total DOS is superimposed
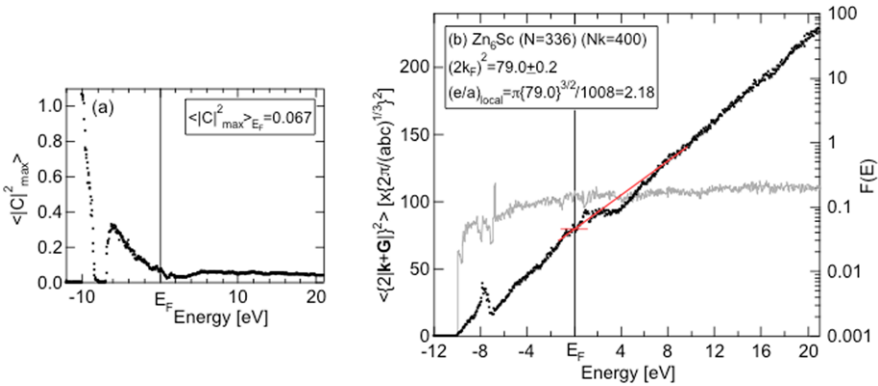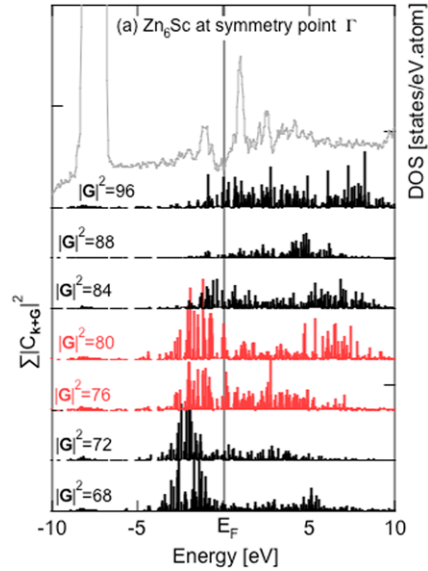

Fig. 15.4 (**a**) Energy dependence of $\langle|C|^2_{\max}\rangle$ and (**b**) Hume–Rothery plot for Zn_6Sc. The ordinate in (**b**) is expressed in units of that in the orthorhombic structure by ignoring a slight deviation of an angle g from 90° in the monoclinic structure [12]. $F(E)$ represents non-dimensional standard deviation [14]

well with the *critical* $|\mathbf{G}|^2$s $= 76$ and 80 mentioned above. This explains the origin of the pseudogap at the Fermi level in terms of Fs–Bz interactions involved.

The effective $\mathbf{e}/\mathbf{a}$ value can be immediately calculated by inserting $(2k_F)^2$ obtained above into $\mathbf{e}/\mathbf{a} = [\pi\{(2k_F)^2\}^{3/2}]/3N$, where N is the number of atoms per unit cell. It turns out to be 2.18, in a good agreement with a composition average of 2.14 under the condition that $(\mathbf{e}/\mathbf{a})_{Zn} = 2.0$ and $(\mathbf{e}/\mathbf{a})_{Sc} = 3.0$. We showed that the matching condition for Cd_6Ca approximant containing 168 atoms per cubic cell is satisfied with $(2k_F)^2 = |\mathbf{G}|^2 = 50$ [15]. An insertion of $\mathbf{e}/\mathbf{a} = 2.18$ and $N = 168$ in
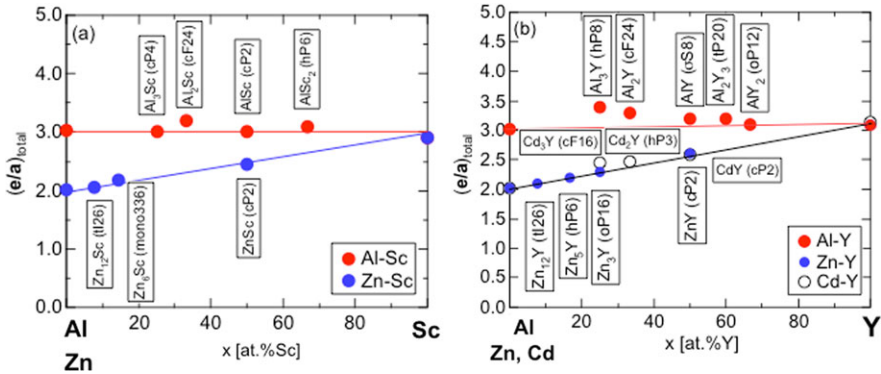
Fig. 15.5 (**a**) Sc and (**b**) Y concentration dependence of $(e/a)_{total}$ for intermetallic compounds in the M–Sc and M–Y (M = Al, Zn and Cd) alloy systems, respectively

place of $N = 336$ back to the equation above results in $(2k_F)^2 = 50$. Hence, we can say that both Zn_6Sc forming a superlattice with $N = 336$ and Cd_6Ca approximant are isoelectronic and obey the Hume–Rothery stabilization mechanism.

It is of great importance to study the universality for the assignment of $(e/a) = 3.0$ for Sc and Y in Group 3. The FLAPW-Fourier analysis and the Hume–Rothery plot were made for existing intermetallic compounds [16] and pure elements in the M–Sc (M = Al and Zn) and M–Y (M = Al, Zn and Cd) alloy systems. We respectively show in Figs. 15.5(a) and (b) the TM concentration dependences of e/a values deduced from the Hume–Rothery plot for all intermetallic compounds mentioned above. The data points for M–Sc (M = Al and Zn) fall on straight lines connecting $(e/a)_{Al} = 3.0$, $(e/a)_{Zn} = 2.0$ and $(e/a)_{Sc} = 3.0$. Similarly, the data for M–Y (M = Al, Zn and Cd) fall on a straight line connecting $(e/a)_{Al} = 3.0$, $(e/a)_{Cd} = 2.0$ and $(e/a)_Y = 3.1$. We conclude that $e/a = 3.0$ and 3.1, respectively, are assigned to TM elements Sc and Y in Group 3 in the periodic table, regardless of their concentrations in M–TM (M = Al, Zn, Cd) alloy systems and that Zn_6Sc with a giant cell does obey this simple rule.

References

1. Tsai AP, Inoue A, Yokoyama Y, Masumoto T (1990) Mater Trans Jpn Inst Met 31:98
2. Yokoyama Y, Tsai AP, Inoue A, Masumoto T, Chen HS (1991) Mater Trans Jpn Inst Met 32:421
3. Raynor GV (1949) Prog Met Phys 1:1
4. Tsai AP, Guo JQ, Abe E, Takakura H, Sato TJ (2000) Nature 408:538
5. Kaneko Y, Arichika M, Ishimasa T (2001) Philos Mag Lett 81:777

6. Andrusyak RI, Kotur BYa, Zavodnik VE (1989) Kristallografiâ 34:996
7. Ishimasa T, Kaneko Y, Kaneko H (2004) J Non-Cryst Solids 334– 335:1
8. Pauling L (1960) The nature of the chemical bond, 3rd edn. Cornell University Press, Ithaca
9. Mizutani U (2010) Hume–Rothery rules for structurally complex alloy phases. CRC Press/Taylor & Francis Group, Boca Raton
10. Inukai M, Zijlstra ES, Sato H, Mizutani U (2011) Philos Mag 91:4247
11. Mizutani U, Inukai M, Sato H, Zijlstra ES (2012) Philos Mag 92:1691
12. Ishimasa T, Kasano Y, Tachibana A, Kashimoto S, Osaka K (2007) Philos Mag 87:2887
13. Blaha P, Schwarz K, Madsen G, Kvasnicka D, Luitz J (2012) WIEN2k. http://www.wien2k.at/, last accessed on August 12, 2012
14. Mizutani U, Inukai M, Sato H, Zijlstra ES (2012) Chem Soc Rev 41:6799
15. Mizutani U, Inukai M, Sato H, Nozawa K, Zijlstra ES (2012) Presented at aperiodic 2012
16. Villars P (1997) Pearson's handbook, crystallographic data. ASM, Materials Park